American Mineralogist, Volume 79, pages 589–605, 1994

Repeating patterns in mineral energetics*

ALEXANDRA NAVROTSKY
Department of Geological and Geophysical Sciences and Princeton Materials Institute, Princeton University, Princeton, New Jersey 08544, U.S.A.

ABSTRACT

Several recurring themes emerge from years of study of the thermodynamics of mineralogical and ceramic systems. These common features are as follows: (1) acid-base interactions determine the energetics of formation of crystals, glasses, and melts; (2) entropy terms arising from configurational, vibrational, and electronic factors are important at high temperature and pressure; (3) in many cases, short-range interactions and local order dominate energetics; and (4) structural states at high temperature and pressure are often not quenchable to ambient conditions, making in-situ study essential for a reliable picture of mineral properties under conditions within the crust and mantle. Examples illustrating each of these themes are presented. The relations among microscopic interatomic interactions and macroscopic physical properties are crucial to understanding processes on a geologic scale.

INTRODUCTION

It is a great pleasure and honor to culminate my year as President with this address. Were I a crystallographer, speaking of repeating patterns would seem natural. In mineral thermodynamics, certain themes emerge so often in diverse systems that they too form repeating patterns. These serve as principles governing the linkage between crystal chemistry and macroscopic stability. Taking examples largely from the work of my research group over the past twenty years, I wish to present and illustrate these recurring commonalities. The relation between microscopic and macroscopic properties, how structure and bonding on an atomic level determine physical and thermodynamic properties has always fascinated me. Process at the geologic scale is dictated by material properties on the atomic scale. The Los Angeles earthquake and the explosion of Mount Saint Helens both involve, as fundamental steps, the ripping apart of strong chemical bonds such as Si-O linkages. Earth science is concerned with process over a bewildering range of distance and time scales. The trends described below help to systematize observations and to provide a semiquantitative predictive framework for the behavior one might expect of minerals encountered in geochemical environments ranging from sediments to the lower mantle.

REPEATING PATTERNS

Opposites attract: Acid-base chemistry dominates in determining enthalpies of formation of interoxidic compounds

The magnitudes of energy encountered in mineral reactions are illustrated in Table 1. It is obvious that the enthalpies associated with petrologically important phase equilibria involving solid-solid reactions or melting are small in magnitude: $<0.5\%$ of a typical lattice energy and $<5\%$ of the enthalpy of formation of the corresponding oxides from the elements. These small differences in enthalpy for competing phase assemblages set the stage for the richness of polymorphism (including high-pressure phase transitions) and the complexity of phase relations encountered in geological and ceramic systems. The small ΔH values also allow entropy, as a T-S term, and pressure, as a P-V term, to influence strongly phase stability, since, at equilibrium at high pressure and temperature,

$$\Delta G(P,T) = \Delta H(1\text{ atm},T) - T\Delta S(1\text{ atm},T) + \int_{1\text{ atm}}^{P} \Delta V(P,T)\,dP \quad (1)$$

or, if $\Delta V(P,T)$ is constant,

$$\Delta G(P,T) = \Delta H^0 - T\Delta S^0 + P\Delta V^0. \quad (2)$$

The enthalpy of formation of $BaCO_3$ from BaO and CO_2 is much more exothermic than that of Al_2SiO_5 from Al_2O_3 and SiO_2, whereas that of Mg_2SiO_4 from MgO and SiO_2 has an intermediate value (see Table 1). Qualitatively, this can be explained readily by BaO being a very basic oxide, CO_2 being a very acidic one, MgO being slightly basic, and Al_2O_3 and SiO_2 both being slightly acidic. An acidic oxide is an oxide ion acceptor, and a basic oxide is an oxide ion donor. Thus the transfer of an oxide ion from BaO to CO_2 to form a Ba^{2+} ion and a CO_3^{2-} ion represents a strong (highly exothermic) acid-base reaction.

It is relatively easy to arrange oxides in a qualitative order of increasing acidity and to group them as basic, amphoteric, and acidic (see Table 2). The ionic potential (z/r) of the cation is a good qualitative and semiquanti-

* Adapted from the Presidential Address given at the annual meeting of the Mineralogical Society of America, October 26, 1993, in Boston, Massachusetts.

0003–004X/94/0708–0589$02.00

TABLE 1. Magnitudes of energies for various reactions

Compounds	Property	ΔH (kJ/mol)
Mg_2SiO_4 (ol)	lattice energy	−20632.1*
Mg_2SiO_4 (ol)	enthalpy of formation from elements	−2170.41**
Mg_2SiO_4 (ol)	enthalpy of formation from oxides	−56.61**
Mg_2SiO_4 (ol)	enthalpy of fusion	114†
Mg_2SiO_4	enthalpy of transition, olivine = β phase	29.9‡
Mg_2SiO_4	enthalpy of transition, β phase = spinel	9.1‡
$BaCO_3$	enthalpy of formation from the oxides	−269.21**
Al_2SiO_5 (kyanite)	enthalpy of formation from the oxides	−5.31**
Al_2SiO_5	enthalpy of transition, kyanite = andalusite	+4.21**

* Ottonello (1987).
** Robie et al. (1978).
† Navrotsky et al. (1989).
‡ Akaogi et al. (1989).

tative measure of basicity. A rough grouping can be made as follows: $z/r < 2$, strongly basic; $2 \leq z/r < 4$, basic; $4 < z/r < 7$, amphoteric; $z/r > 7$, acidic. The most stable compounds are then formed by combining a very acidic and a very basic oxide. Figure 1 shows the enthalpies of formation of a series of aluminates, silicates, tungstates, and carbonates. As acidity increases in the order Al, Si, W, C, the compounds become more stable, and their structures contain increasingly well defined complex discrete anions. As the divalent ion varies, the heat of formation of a given series of compounds (e.g., orthosilicates) becomes more exothermic with decreasing ionic potential of the cation (see Fig. 2). The transition metal compounds have less exothermic heats of formation than would be predicted from this trend (see Fig. 2). Both the general trend and the deviation of the transition metals from it can be rationalized in terms of the completeness of oxide ion transfer from the divalent cation to the multivalent cation, in the sense that smaller size and greater covalency both act to increase bonding between the divalent ion and O, and the oxide ion transfer (Lux-Flood basicity) can be thought of as reflecting the competition of the two types of ions (Si^{4+} and M^{2+}) for the O atom's electron density.

Similar trends are seen in melts and glasses. In binary metal oxide-silica systems, the thermodynamic mixing properties are dominated by the major acid-base reaction: the transfer of oxide ion from metal oxide to silica. This is a depolymerizing reaction, forming two nonbridging Si-O bonds from one Si-O-Si linkage. The more basic the oxide (smaller z/r), the more complete the oxide ion transfer, and, for a given composition, the more depolymerized and less viscous the melt. These trends are reflected in the enthalpies of mixing in binary molten silicates (see Fig. 3). Note the rather large enthalpies involved (up to −100 kJ/mol), the maximum stabilization near orthosilicate composition, and the increase in stabilization with the increasing basicity of the metal oxide, i.e., in the order Pb, Ca, Na, K (Navrotsky, 1986).

TABLE 2. Acid-base scales for oxides

Oxide[A]	z/r of cation	Optical basicity	Enthalpy of solution (kJ/mol) B	C	D
K_2O	0.66[E]	1.4[F]	−282[G]		
Na_2O	0.89	1.15	−176		
BaO	1.45	1.15	−127	−87.9	
SrO	1.59		−93.6	−59.2	
CaO	2.00	1.0	−58.0	−23.5	−37.1
MnO	2.41		5.4		
FeO	2.56		16.0		
$\frac{1}{3}La_2O_3$	2.58		−42.6		
CoO	2.68		23.0		−20.5
$\frac{1}{3}Nd_2O_3$	2.71		−28.4		
CuO	2.74		33.0		11.1
MgO	2.77	0.76	−4.8	−25.9	
$\frac{1}{3}Sm_2O_3$	2.78		−26.5		
$\frac{1}{3}Eu_2O_3$	2.81		−22.1		
$\frac{1}{3}Gd_2O_3$	2.85		−24.2		
NiO	2.90		37.0		−3.2
$\frac{1}{3}Dy_2O_3$	2.92		−17.0		
$\frac{1}{3}Y_2O_3$	2.94		−20.6		
$\frac{1}{3}Ho_2O_3$	2.96		−16.7		
$\frac{1}{3}Er_2O_3$	2.99		−15.9		
$\frac{1}{3}Tm_2O_3$	3.02		−15.7		
$\frac{1}{3}Yb_2O_3$	3.05		−13.2		
$\frac{1}{3}Lu_2O_3$	3.07		−11.44		
ZnO	3.33		17.9	−13.4	
$\frac{1}{3}Sc_2O_3$	3.45		−0.6		
$\frac{1}{3}Fe_2O_3$	4.65		26.7		−1.1
$\frac{1}{2}ZrO_2$	4.76			22.2	
$\frac{1}{3}Ga_2O_3$	4.84		18.0		
$\frac{1}{3}Cr_2O_3$	4.88		11.2		
$\frac{1}{3}Mn_2O_3$	5.17				34.6
$\frac{1}{3}Al_2O_3$	5.60	0.605	11.0	30.0	
$\frac{1}{2}TiO_2$	6.61		10.8	19.6	5.3
BeO	7.41		14.4		
$\frac{1}{2}GeO_2$	7.55		1.0		
$\frac{1}{3}WO_3$	14.3				10.1
$\frac{1}{3}MoO_3$	14.6				3.3
$\frac{1}{2}SiO_2$	15.4	0.48	−1.8	−6.0	

[A] The z/r increases downward in the table, indicating a general increase in acidity.
[B] In molten $2PbO \cdot B_2O_3$ near 973 K.
[C] In molten $0.52LiBO_3 \cdot 0.42NaBO_3$ near 1050 K.
[D] In molten $3Na_2O \cdot 4MoO_3$ near 973 K.
[E] Ionic radius taken from Shannon (1976) for the coordination number in the polymorph stable at 973 K and 1 atm.
[F] Duffy and Ingram (1971a).
[G] Uncertainties are generally $< \pm 2$ kJ. Data are from many different experiments in Navrotsky's work.

The enthalpies associated with the charge-coupled substitution of $M^{n+}_{1/n}AlO_2$ in a framework glass are shown in Figure 4. The process of dissolving an aluminosilicate glass in molten lead borate to form a dilute solution (<1 wt%) breaks up the aluminosilicate framework structure into isolated species, namely, silicate and aluminate tetrahedra and alkali and alkaline-earth cationic species dissolved in a borate matrix. Thus the enthalpy of solution may be considered a measure of the strength of bonding in the aluminosilicate glass, at least in a relative sense, when comparing various compositions. Three points are evident from Figure 4. First, for Al/(Al + Si) < 0.5, the enthalpies of solution generally become more endothermic as $M_{1/n}AlO_2$ is substituted for SiO_2. This increase becomes more pronounced with decreasing z/r (or increasing basicity) in the series Mg, Ca, Sr, Pb, Ba, Li, Na, K, Rb, Cs. Second, for Al/(Al + Si) > 0.5 the enthalpy

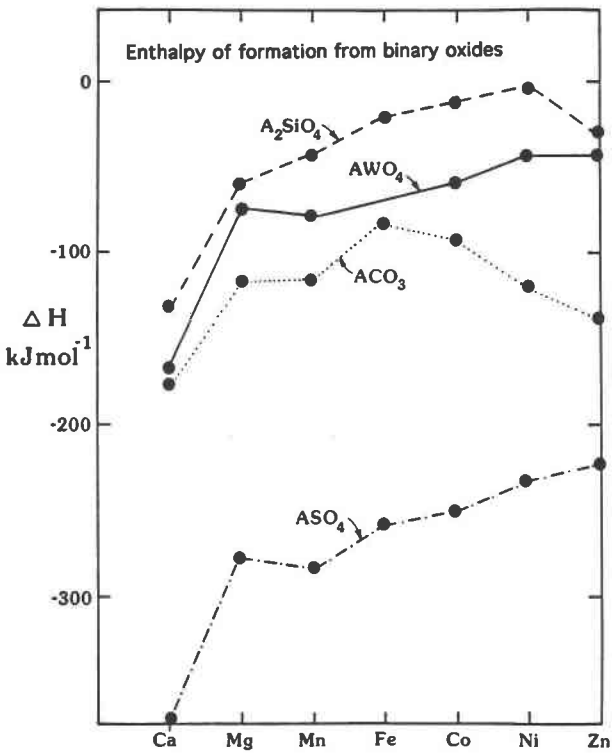

Fig. 1. Enthalpy of formation of a series of aluminates, silicates, tungstates, and carbonates from the oxides. Data are from Navrotsky and Kleppa (1968, 1969), and Navrotsky (1971, 1974).

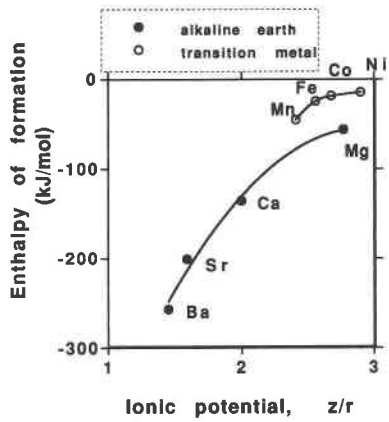

Fig. 2. Enthalpy of formation of orthosilicates vs. ionic potential (z/r) of divalent cations.

of solution curves bend back toward more exothermic values, with a maximum near 0.5. This behavior is seen most clearly in the calcium aluminate–silica system, in which data exist for compositions ranging to virtually pure $Ca_{0.5}AlO_2$ (see Fig. 5), and is suggested in the sodium aluminate–silica system. This maximum reflects an exothermic enthalpy of mixing for the reaction

$$xM_{1/n}AlO_2 + (1 - x)SiO_2 = M_xAl_xSi_{1-x}O_2 \qquad (3)$$

in glasses, which parallels, but is smaller in magnitude than, the corresponding enthalpy of formation in the crystalline state (see Fig. 5). Third, at high silica content, pronounced curvature occurs in the relations for the alkaline-earth elements. This curvature suggests a positive heat of mixing in this region and may presage glass-glass immiscibility.

The enthalpy of Reaction 3 becomes more exothermic with increasing basicity of the oxide $M^{n+}_{1/n}O$ (decreasing field strength, z/r, of the cation M) (see Fig. 6). The energetics can also be correlated in terms of the perturbation of T-O-T bond lengths and angles, both as observed in crystalline aluminosilicates and as calculated by molecular orbital methods (Geisinger et al., 1985; Navrotsky et al., 1985).

Despite clear qualitative trends, relating energetics and acid-base character quantitatively is difficult. There has been some success in predicting enthalpies of formation of minerals using a scheme that parameterizes the contribution of various ionic species to the enthalpy of hydrous silicates (e.g., Tardy and Garrets, 1974). A similar approach, based on a parameterization of contributions of various polyhedra, has been used to calculate enthalpies and entropies of formation of oxides (Reznitskiy, 1986), standard entropies, heat capacities, and heat contents (Robinson and Haas, 1983). In general, these schemes are moderately successful when the enthalpies of formation are large but do not discriminate well among compounds of lesser stability.

For the study of multicomponent crystals, glasses, and melts, small differences in electronegativity and relatively minor adjustments in the electron distributions related to compound formation are of interest. Thus a scale of relative acidity, easily applied to a variety of ions in a number of environments, is desirable. The concept of optical basicity, developed by Duffy and coworkers (Duffy and Ingram, 1971a, 1971b, 1976; Duffy, 1989), offers a very useful approach. Initially applied to metallurgical slags and glasses, it is now finding much wider use.

When a cation is coordinated by a Lewis base (simple or complex anion), its outer orbitals are profoundly affected. A $d^{10}s^2$ ion like Tl^+ or Pb^{2+}, whose strong ultraviolet $^1S_0 \rightarrow {}^3P_1$ band is very sensitive to changes in the ionic-covalent nature of bonding, serves as a useful probe. With greater covalency, the UV band is shifted to lower energies (red shifted). The quantity Λ is defined as

$$\Lambda = \frac{\nu_i - \nu}{\nu_i - \nu_{O^{2-}}} \qquad (4)$$

in which ν is the frequency of the probe ion in the sample of interest, ν_i is the frequency in the gas phase (where no electron donation is possible), and $\nu_{O^{2-}}$ is the frequency in a reference oxide that is strongly ionic (e.g., CaO). Thus the measurement of basicity is transformed into a fairly straightforward optical spectroscopic measurement on a sample doped with trace amounts of Pb^{2+} or Tl^+. The optical basicities of several oxides are shown in Table 2.

The enthalpy of solution of crystalline oxides in molten

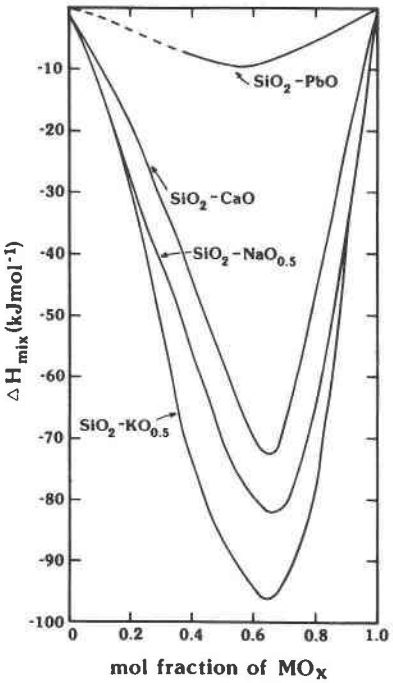

Fig. 3. Enthalpy of mixing in binary molten silicates.

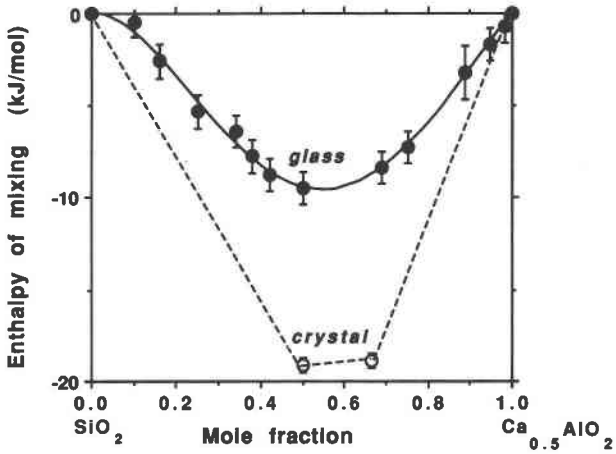

Fig. 5. Enthalpy of formation of crystalline and glassy calcium aluminosilicates from SiO_2 and $Ca_{0.5}AlO_2$ (data from Navrotsky et al., 1982). Solid circles = glassy phases from glassy end-members; open circles = crystalline phases from crystalline end-members.

oxide solvents, for which a body of data has been amassed through solution calorimetry over the years, forms a semiquantitative measure of acid-base character. Because a basic oxide (e.g., BaO) can donate oxide ions to the borate or molybdate species in the melt, increasingly exothermic heats of solution are seen with decreasing z/r (see Table 2 and Fig. 7). Amphoteric oxides (e.g., Al_2O_3) show endothermic heats of solution, whereas the enthalpies of solution of acidic oxides (e.g., SiO_2) become slightly exothermic because they can abstract oxide ions from the solvent to form complex anions, such as SiO_4 groups. The solvent itself has been tailored to be a buffer containing a mixture of borate or molybdate species so that it can readily dissolve both basic and acidic oxides. The three solvents for which the most data exist (see Fig. 7) are $2PbO \cdot B_2O_3$ near 973 K, $3Na_2O \cdot 4MoO_3$ near 973 K, and $0.48NaBO_3 \cdot 0.52LiBO_3$ near 1050 K. Although the values of heat of solution of a given oxide differ somewhat in each solvent, the overall trends in Figure 7 are remarkably similar, so that the data are to a first approximation described by a single curve, going from strongly exothermic values for very basic oxides ($z/r < 2$), moderately endothermic values for oxides of intermediate basicity, and slightly exothermic values for acidic oxides. This approximately single trend reflects that the three solvents chosen probably represent a fairly similar acid-base character. The rare-earth oxides show moderate exothermic heats of solution, whereas the transition metal oxides with similar z/r show moderate endothermic effects. This may reflect covalency and d-electron behavior for the latter. Comparing the borate solvents in more detail, one sees in the alkali borate somewhat more endothermic heats of solution for the basic alkaline-earth oxides but a more exothermic heat of solution for the acidic oxide, quartz, than in the lead borate. This suggests that $0.52LiBO_3 \cdot 0.48NaBO_3$ is slightly more basic than $2PbO \cdot B_2O_3$. This greater basicity reflects the smaller z/r of Li compared with Pb.

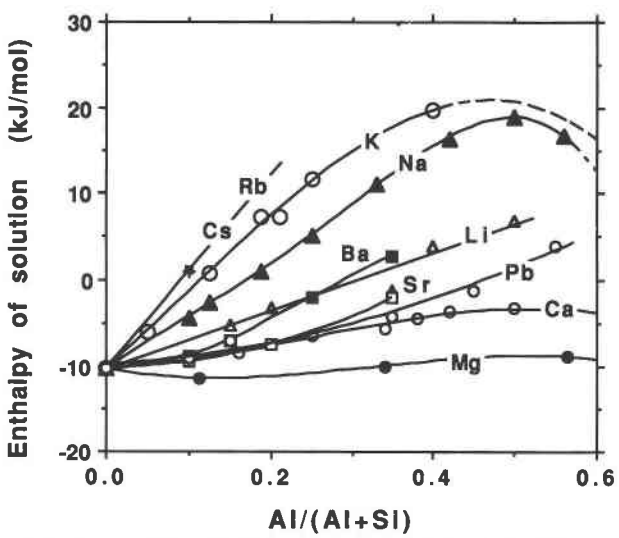

Fig. 4. Enthalpy of solution in molten $2PbO \cdot B_2O_3$ of glasses along SiO_2-$M^{n+}_{1/n}AlO_2$ joins (Roy and Navrotsky, 1984).

A little entropy goes a long way: The $T\Delta S$ term is very influential in mineral stability at high temperature

There are three major sources of entropy changes in mineral reactions in the solid state: configurational entro-

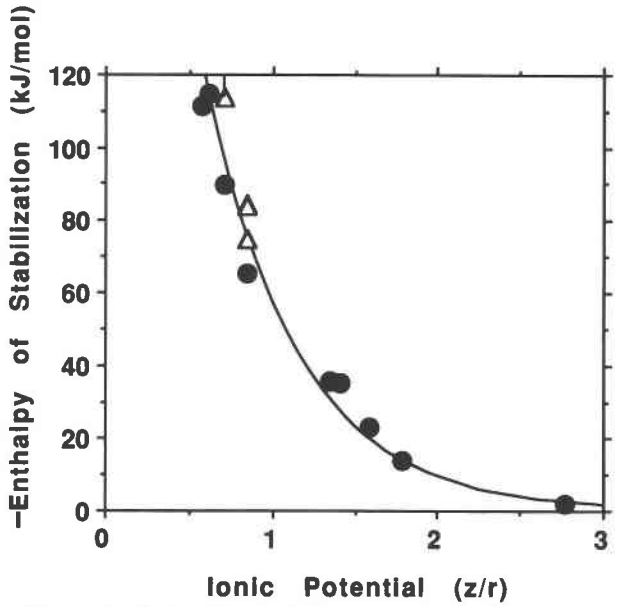

Fig. 6. Enthalpy of coupled substitution $Si^{4+} = Al^{3+} + 1/_nM^{n+}$ in crystals (triangles) and glasses (circles) vs. z/r of M^{n+} (data from Navrotsky et al., 1985).

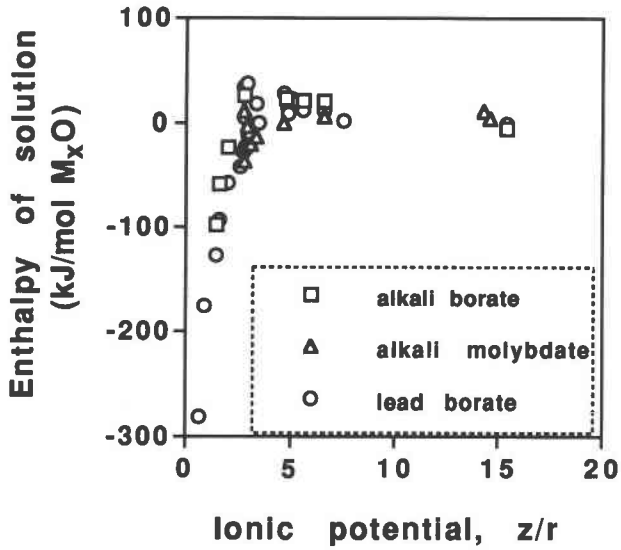

Fig. 7. Enthalpy of solution (in kilojoules per mole of M_xO, so that the transfer of 1 mol of oxide ion is involved) of crystalline oxides in molten oxide solvents, plotted against ionic potential, z/r (radius chosen for the coordination number of ion in the crystal). Squares represent ΔH_{sol} in molten $0.52LiBO_3 \cdot 0.48NaBO_3$ near 1050 K, triangles molten $3Na_2O \cdot 4MoO_3$ near 973 K, circles molten $2PbO \cdot B_2O_3$ near 973 K. Uncertainty in ΔH_{sol} values is generally $< \pm 2$ kJ.

py resulting from positional disorder, vibrational entropy resulting from differences in the distribution of vibrational frequencies (the vibrational density of states), and electronic entropy resulting from changes in electronic state (including electron spin, electron delocalization and magnetic effects). Although these factors are not rigorously separable, they can often be treated independently as a first approximation, and each can be important in determining mineral stability.

The zero-point entropy resulting from cation disorder is familiar to mineralogists. For a simple case in which several distinguishable chemical species (ions), i, are distributed over 1 mol of sites, the configurational entropy has the form

$$S_{conf} = -R \sum_i X_i \ln X_i. \quad (5)$$

S_{conf} is shown in Figure 8. This entropy, which also represents the entropy of mixing of an ideal one-site solid solution, is symmetric about $X = 0.5$ and rises steeply, with initially vertical slope (implying infinite partial molar entropy of the solute at infinite dilution) at both ends of the composition range. For more complex stoichiometries, charge-coupled substitutions, and cases with strong short-range order, the configurational entropy takes on more complex forms (see, for example, Hon et al., 1981; Capobianco et al., 1987), but some logarithmic term persists. This term assures that the initial stages of admixture or disordering produce a larger contribution to the entropy than small changes in composition or structural state in an already highly disordered system. This behavior in turn implies that, at high temperatures, all impurities have a finite solubility in all phases and all conceivable defects have an equilibrium concentration. Whether the concentration of a particular defect is parts per million or several percent depends on the magnitude of the ΔH that needs to be balanced by the $T\Delta S$ term. But the point to remember is that every such incorporation reaction will initially lower the free energy of each phase, and the free energy

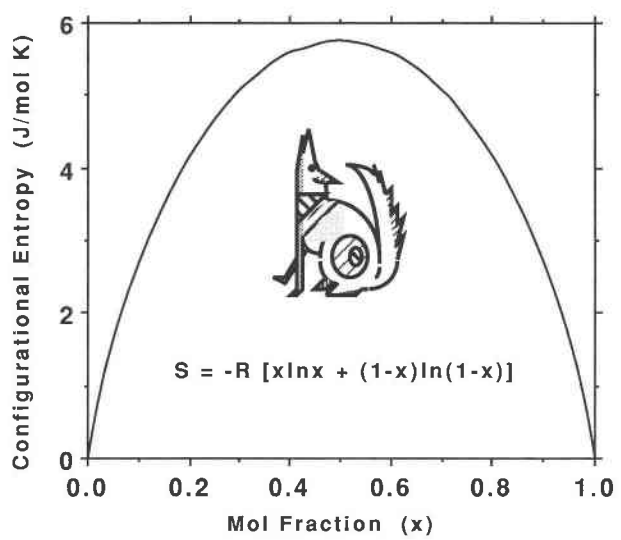

Fig. 8. Configurational entropy for a binary system, A-B, mixing 1 mol of ions over 1 mol of sites $S_{conf} = -R[X \ln X + (1 - X)\ln(1 - X)]$, where X is the one independent mole fraction. Coyote the Trickster, shown here, embodies quintessential entropy.

TABLE 3. Entropy-stabilized compounds

System	Decomposition reaction	ΔH (kJ/mol)	ΔS [J/(mol·K)]	Temperature below which decomposition occurs (K)
	Pseudobrookite: M-site disorder			
Fe_2TiO_5*	$Fe_2TiO_5 = Fe_2O_3 + TiO_2$	−8.3	−9.9	838
Al_2TiO_5*	$Al_2TiO_5 = Al_2O_3 + TiO_2$	exothermic		1273
Ga_2TiO_5*	$Ga_2TiO_5 = Ga_2O_3 + TiO_2$	exothermic		1273
$FeTi_2O_5$*	$FeTi_2O_5 = FeTiO_3 + TiO_2$			1430
$MgTi_2O_5$*	$MgTi_2O_5 = MgTiO_3 + TiO_2$	−9.8	−12	823
$CoTi_2O_5$*	$CoTi_2O_5 = CoTiO_3 + TiO_2$	−26.6	−19	1400
	Spinels: Tetrahedral-octahedral disordering			
$CuAl_2O_4$**	$CuAl_2O_4 = CuO + Al_2O_3$	−24.6		
$CuFe_2O_4$**	$CuFe_2O_4 = CuO + Fe_2O_3$	−21.1		
$CdFe_2O_4$**	$CdFe_2O_4 = CdO + Fe_2O_3$	−7.4		
$CuGa_2O_4$**	$CuGa_2O_4 = CuO + Ga_2O_3$	−16.6		
$NiMn_2O_4$**	$NiMn_2O_4 = NiO + Mn_2O_3$	−2.0		
$CuMn_2O_4$**	$CuMn_2O_4 = CuO + Mn_2O_3$	−16.7		
	Mullite: Al, Si, and O, vacancy disorder			
$Al_6Si_2O_{13}$†	$Al_6Si_2O_{13} = 3Al_2O_3 + 2SiO_2$	−50		
	Spinelloids			
$NiAl_2O_4$-Ni_2SiO_4: disorder over several octahedral and tetrahedral sites				
$0.75NiAl_2O_4$-$0.25Ni_2SiO_4$ (I)‡	$I = 0.75NiAl_2O_4$ (sp) + $0.25Ni_2SiO_4$ (sp)	−4.0	−5.0	800
$0.60NiAl_2O_4$-$0.40Ni_2SiO_4$ (II)‡	$II = 0.60NiAl_2O_4$ (sp) + $0.40Ni_2SiO_4$ (sp)	−4.5	−5.0	900
$0.5NiAl_2O_4$-$0.5Ni_2SiO_4$ (III)‡	$III = 0.5NiAl_2O_4$ (sp) + $0.5Ni_2SiO_4$ (sp)	−9.4	−6.15	1450
$0.5NiAl_2O_4$-$0.5Ni_2SiO_4$ (IV)‡	$IV = 0.5NiAl_2O_4$ (sp) + $0.5Ni_2SiO_4$ (sp)	−9.4	−9.5	990
$0.5NiAl_2O_4$-$0.5Ni_2SiO_4$ (V)‡	$V = 0.5NiAl_2O_4$ (sp) + $0.5Ni_2SiO_4$ (sp)	−14.9	−13.0	1150
$MgGa_2O_4$-Mg_2GeO_4				
$0.5MgGa_2O_4$-$0.5Mg_2GeO_4$ (β)§	$\beta = 0.5MgGa_2O_4$ (sp) + $0.5Mg_2GeO_4$ (sp)	−10.8		
	Brownmillerite: Fe,Ti octahedral disorder			
$Ca_2Fe_2TiO_8$§	$Ca_2Fe_2TiO_8 = Ca_2Fe_2O_5 + CaTiO_3$	−2.2	−11.5	190
$Ca_4Fe_2Ti_2O_{11}$§	$Ca_4Fe_2Ti_2O_{11} = Ca_2Fe_2O_5 + 2CaTiO_3$	−14.0	−15.9	880

* Navrotsky (1975).
** Navrotsky and Kleppa (1968).
† Gerardin et al. (1994).
‡ Akaogi and Navrotsky (1984). Note these are high-pressure reactions; this decomposition is predicted but has not been observed and is metastable with respect to other phase changes.
§ Prasanna and Navrotsky (1994).

is minimized when all defects are at their equilibrium concentrations. Thus a little entropy goes a long way, and rocks, formed in high-temperature environments with the whole periodic table in natural abundances as feedstock, are guaranteed to be complex on the atomic scale.

A first-order consequence of massive configurational disorder, which occurs when crystallographically distinct sites are energetically similar for several ionic species, is the stabilization at high temperature of phases that have positive enthalpies of formation from binary oxides or from other phase assemblages. I refer to these as entropy-stabilized compounds, because the driving force for their formation is the $T\Delta S$ term rather than ΔH. Such phases are stable only above some temperature at which $\Delta H = T\Delta S$. Cases of entropy-stabilized phases, that are taken for granted include all high-temperature polymorphs and the molten state. Examples of entropy-stabilized compounds for which configurational disorder provides the entropy are shown in Table 3. They span a variety of structure types. An interesting group includes ordered phases of marginal stability in a pseudobinary system, e.g., spinelloids along the $NiAl_2O_4$-Ni_2SiO_4 and $MgGa_2O_4$-Mg_2GeO_4 joins (Akaogi and Navrotsky, 1984; Leinenweber and Navrotsky, 1989) and brownmillerite-related phases along the $CaFe_2O_5$-$CaTiO_3$ join (Prasanna and Navrotsky, 1994). Although energetically less favorable than a mixture of end-members, these are stable with respect to end-members, to neighboring phases, and to a hypothetical, continuous solid solution.

Spinels, AB_2O_4, provide a classic example of the interplay of energetics and structure. The spinel stoichiometry provides two octahedral and one tetrahedral cation site per four O atoms, and cation distributions ranging from normal $^{[4]}A^{[6]}B_2O_4$ to inverse $^{[4]}B^{[6]}(AB)O_4$ are known. The configurational entropy (if one assumes no short-range order on either the tetrahedral or the octahedral sublattice) for a degree of disorder, x, in $^{[4]}(A_{1-x}B_x)^{[6]}(A_xB_{2-x})O_4$ is given by

$$S_{conf} = -R[x \ln x + (1 - x)\ln(1 - x) + x \ln(\tfrac{1}{2}) + (2 - x)\ln(1 - \tfrac{x}{2})]. \quad (6)$$

This function is shown in Figure 9. S_{conf} is a maximum at the random distribution, $x = \frac{2}{3}$. Initial disordering of a fully normal spinel, with $S_{conf} = 0$ at $x = 0$, increases the entropy more sharply than the disordering of an inverse spinel, with $S_{conf} = 2R \ln 2$ at $x = 1$. Both normal

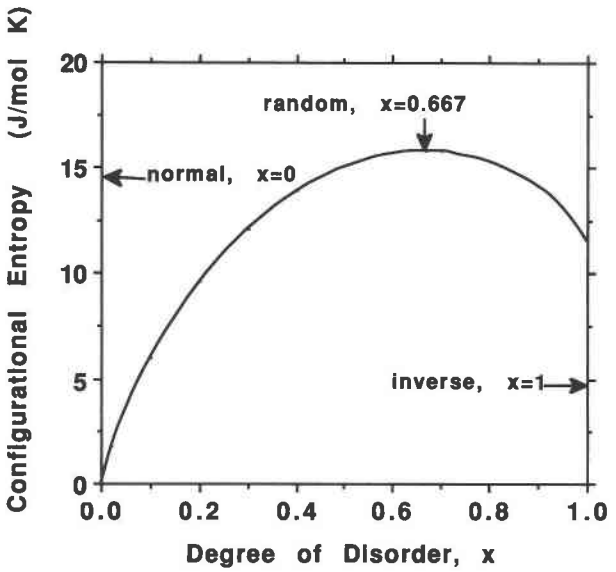

Fig. 9. Configurational entropy of a system having two sites of one kind and one of another (e.g., spinel, pseudobrookite, melilite) vs. the degree of disorder, x (Eq. 6).

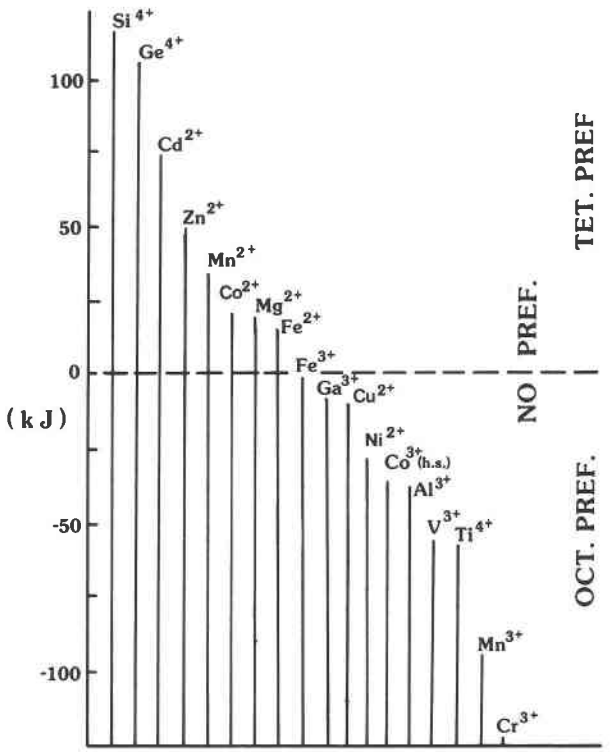

Fig. 10. Site preference energies of cations in spinels (O'Neill and Navrotsky, 1983).

and inverse spinels generally become disordered toward the random distribution as temperature increases.

The disordering equilibrium may be written as the reaction

$$^{[4]}A + {}^{[6]}B = {}^{[6]}A + {}^{[4]}B \quad (7)$$

The equilibrium constant for this reaction is

$$K = x^2/[(1 - x)(2 - x)] \quad (8)$$

and the free energy of disordering is

$$\Delta G_{dis} = \Delta H_{dis} - T\Delta S_{dis} = -RT \ln K. \quad (9)$$

Several models have been applied to calculate ΔG_{dis}. The simple equilibrium model of Navrotsky and Kleppa (1967) equates ΔS with the configurational entropy of disordering and sets ΔH directly proportional to the degree of disorder, x, with the proportionality constant, which represents the interchange enthalpy, being a difference of site preference energies of the ions involved. O'Neill and Navrotsky (1983, 1984) modified this model to give the interchange enthalpy a linear dependence on the average charge on the octahedral sublattice. This gives ΔH_{dis} a quadratic dependence on x, but the model can be applied in such a way as to preserve the concept of a site preference energy (see Fig. 10). This two-parameter formalism is suggested by lattice energy considerations. It does a better job than the simple model in describing experimental cation distribution data, particularly in solid solutions between a normal and an inverse spinel. Coupled with bond length considerations, this model offers an explanation of otherwise anomalous sigmoidal variations in lattice parameters in spinels such as chromite-magnetite and of activity-composition relations in this and other systems (O'Neill and Navrotsky, 1984). The point to note is that seemingly complex behavior in physical and thermodynamic properties is a direct consequence of the form of the configurational entropy (Eq. 6) combined with rather straightforward energetics.

Cation distribution equilibria are further complicated by kinetic factors. At low temperature, these reactions occur too sluggishly for equilibrium to be attained; a structural state representative of some closure temperature is frozen in. At high temperature, disorder might not be quenchable on a laboratory time scale (see below).

Electronic transitions generally occur rapidly and reversibly. An example is shown in Figure 11; the excess heat capacity of Co_3O_4 spinel signals a transition from low-spin to high-spin Co^{3+} (Mocala et al., 1992). The randomization of the cation distribution in magnetite at high temperature represents rapid electron hopping. At high pressure, changes in the electronic state of Fe^{2+} may become important, especially in FeO under lower mantle conditions.

Changes in vibrational entropy play a significant role in high-pressure phase transitions. In the Earth's deep interior, the change in Si coordination from tetrahedral to octahedral occurs in the reaction believed to be responsible for the 660-km seismic discontinuity separating the transition zone from the lower mantle.

$$\underset{\text{spinel}}{(Mg,Fe)_2SiO_4} = \underset{\text{perovskite}}{(Mg,Fe)SiO_3} + \underset{\text{rock salt}}{(Mg,Fe)O}. \quad (10)$$

The Clapeyron slope, dP/dT, of this transition is one of the factors that determine whether whole-mantle convection, two layer convection, or intermittent slab and plume

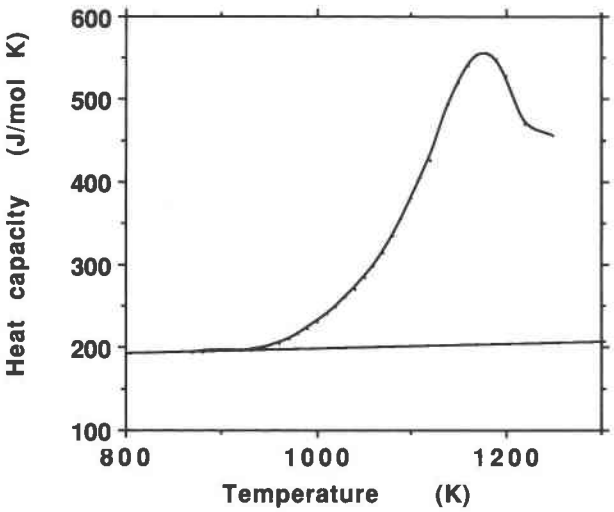

Fig. 11. Heat capacity of Co_3O_4 spinel (Mocala et al., 1992).

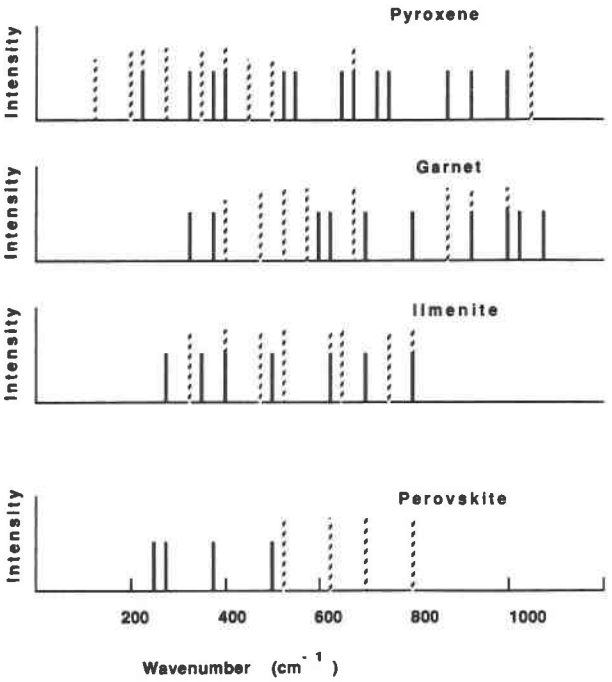

Fig. 12. Schematic representation of infrared (dotted) and Raman (solid) peaks in vibrational spectra of $MgSiO_3$ polymorphs. Heights of lines have no significance (from Navrotsky, 1994).

penetration predominates in the Earth. A strongly negative Clapeyron slope hinders mass transport across the 660-km discontinuity. Navrotsky (1980) suggested that lower mantle phase transitions may generally have negative P-T slopes. $MgSiO_3$ perovskite, the high-pressure phase, would have an anomalously large vibrational entropy, both because the octahedral Si-O bond is weaker than the tetrahedral and because Mg occupies a rather large eightfold-coordinated site. Thus the style of mantle convections is linked to changes in the vibrational density of states.

These ideas can be made more quantitative by applying the lattice dynamical modeling of Kieffer (1979a, 1979b, 1979c, 1979d, 1982) to the $MgSiO_3$ polymorphs at high pressure (Navrotsky, 1988; Fei et al., 1990). This approach treats the vibrational density of states as a composite of acoustic modes, Einstein oscillators for identifiable localized vibrations, and an optic continuum, whose extent is consistent with vibrational spectra, for the remaining lattice modes.

Kieffer's approach is particularly useful for high-pressure phases, which certainly are not available in quantities suitable for low-temperature C_p measurements. The input data needed to constrain the model are space group, molar volume, elastic constants, bulk modulus, thermal expansion, and vibrational (infrared and Raman) spectra. All these data are obtainable for ultrahigh-pressure phases and indeed are of interest to geophysics for other reasons.

Figure 12 shows schematic vibrational spectra for the pyroxene, garnet, ilmenite, and perovskite forms of $MgSiO_3$. Figure 13 shows representative Kieffer-type models consistent with the spectra. Figure 14 shows heat capacities and entropies consistent with these models. The heat capacity and entropy curves show crossovers at low temperature. At high temperature, the order of decreasing entropy is pyroxene, garnet, perovskite, ilmenite, whereas that of increasing density is pyroxene, garnet, ilmenite, perovskite. The complex heat-capacity relations reflect the balance of several factors. With increasing density (smaller unit cell), the entropy will decrease (all other factors being similar). This reflects normal entropy-volume systematics as seen in the α-β-γ transitions. Superimposed on this trend are two other effects. As Si becomes sixfold-coordinated (half is octahedral in garnet, all is octahedral in ilmenite and perovskite), the Si-O stretching vibrations at 900–1100 cm^{-1} of the strongly bonded SiO_4 tetrahedra are transformed to lower frequency vibrations (600–800 cm^{-1}) of SiO_6 octahedra, which are not readily identifiable and form part of the optic continuum. This increases C_p and S^0 at a given temperature and counteracts the effect of increasing density. The low-frequency cutoff of the optic continuum is highest for ilmenite, intermediate for pyroxene and garnet, and lowest for perovskite. Although it is tempting to describe this as increasing rattling of Mg in a larger and more distorted coordination polyhedron, the real dynamical situation is more complex and involves lattice modes rather than localized vibrations. Nonetheless, this effect tends to raise the heat capacity and entropy of perovskite and lower that of ilmenite. Finally, the somewhat larger thermal expansivity of perovskite compared with other phases increases the term for converting C_v to C_p and raises the entropy of perovskite.

Pyroxene is the phase of highest entropy, and ilmenite of the lowest, with garnet and perovskite intermediate. Above 1000 K, perovskite has a slightly higher entropy

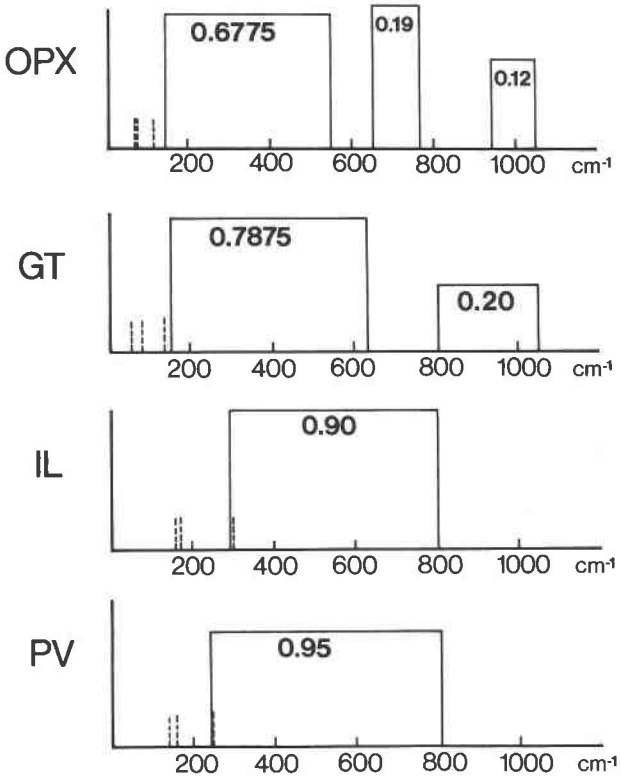

Fig. 13. Schematic representation of the vibrational density of states (excluding acoustic modes and neglecting dispersion) consistent with spectra in Fig. 12 (from Navrotsky, 1994).

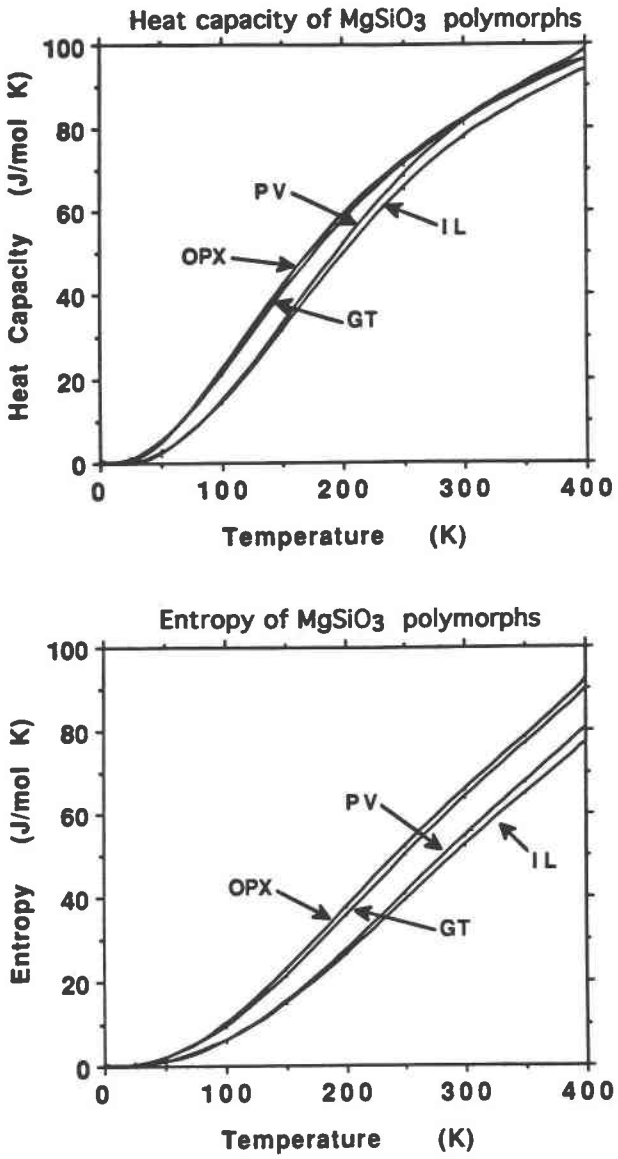

Fig. 14. Calculated values of heat capacity (**top**) and entropy (**bottom**) using vibrational density of states in Fig. 13 (from Navrotsky, 1994).

than garnet. The ilmenite → perovskite transition has a definitely positive ΔS^0 and a negative dP/dT. Above 1000 K, ΔS^0 of phase transitions is virtually independent of temperature.

Figure 15 shows the phase diagram for the $MgSiO_3$ composition, consistent with these calculated entropies, phase equilibria, and calorimetry. Note the negative slope for the perovskite-forming reaction and that $MgSiO_3$ garnet is stable only at very high temperature. This phase, if cubic at high P-T conditions, may be entropy-stabilized by octahedral Mg,Si disorder.

From the above calculations and from experimental observations, one can draw the following general conclusions: For phase transitions involving no changes in cation coordination, ΔS generally scales with ΔV, and phase transitions have positive P-T slopes. The lower entropies of denser phases generally result from small shifts in the vibrational density of states, with the denser phase showing fewer low frequency modes. When a change in coordination occurs, much more pronounced changes are seen in the vibrational spectrum. Since an increase in coordination number lengthens and weakens the bonds in the first coordination sphere (while increasing their number), this change generally implies a shift in the vibrational density of states toward lower frequencies. This shift is especially pronounced when tetrahedral Si-O bonds are converted to octahedral Si-O linkages. The result is that entropy-volume systematics break down, and the denser phase has a substantially higher entropy than otherwise expected and, in extreme cases, has an entropy higher than that of the lower pressure polymorph (e.g., for the ilmenite-perovskite transition). Anomalies in the relation of other physical properties (elastic constants, thermal expansion, compressibility) to density may also occur in phase transitions involving changes in coordination number. Such effects, though especially pronounced in silicates, can be expected to occur for many solid-state systems undergoing phase transitions with changes in nearest neighbor coordination.

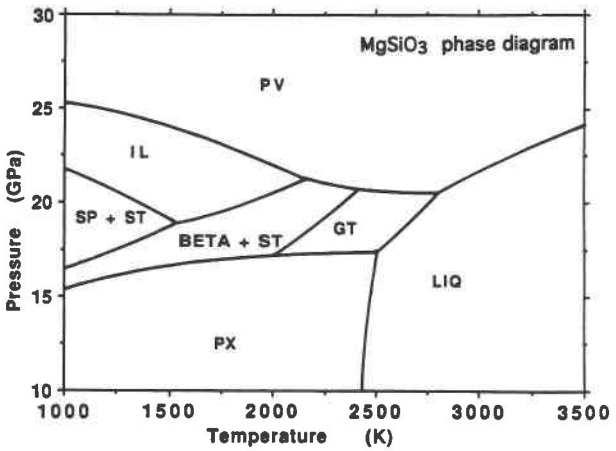

Fig. 15. Phase diagram of $MgSiO_3$ at high pressure and temperature consistent with entropies in Fig. 14 and with calorimetric determinations of enthalpies of transitions (Fei et al., 1990; Ito et al., 1990).

Atoms in a structure, like homeowners in a town, care mostly about their immediate neighbors: Short-range interactions and local order often dominate in determining energetics

Even though oxides and silicates are viewed as largely ionic, with long-range Coulombic forces, the effects of nearest and next-nearest neighbor configurations usually dominate in defining structures and thermodynamic properties. This is manifested in many ways.

Many phase transitions preserve local coordination environments. When such a transition involves only small changes in orientation, articulation of chains, or stacking of layers, the energy involved is very small (see Table 4). Even melting preserves coordination polyhedra and bond lengths to a remarkable degree. Enthalpies of vitrification and of fusion, though larger than enthalpies of many solid-solid transitions, are much smaller than enthalpies of vaporization, and represent at most a few percent of the total lattice energy of the condensed phase. Thus destroying long-range periodicity completely has only a modest energy cost.

Near neighbor configurations dominate effects seen by structural probes such as Raman, infrared, NMR, EXAFS, XANES, and Mössbauer spectroscopy. Because these tools respond to changes in electron distribution about a given atom, their sensitivity to nearest and next-nearest neighbors and their relative insensitivity to longer range correlations imply that the electron density distribution is most sensitive to the nearest and next-nearest neighbor environments. The success of molecular orbital calculations, which model a silicate or other crystal by the configuration of a small molecular cluster (Gibbs, 1982; Geisinger et al., 1985; Navrotsky et al., 1985), also attest to the importance of local geometry. Recent work suggests that even long-range order, including crystal symmetry as well as bond distances and angles in silica polymorphs, can be modeled correctly by simulated annealing procedures on structures for which potentials have been derived from the $H_4Si_2O_7$ molecular cluster (Boisen et al., in preparation).

Table 4. Energetics of phase transitions involving no change in local coordination

Transition	ΔH (kJ/mol)
SiO_2 (β quartz = cristobalite)*	0.9 ± 0.5
Phlogopite (1M = 1Md)**	3.3 ± 4
$MnSiO_3$ (rhodonite = pyroxmangite)†	0.3 ± 0.5
$MnSiO_3$ (pyroxmangite = clinopyroxene)†	1.9 ± 0.5
$CaTiO_3$ (tetragonal = cubic)‡	2.3 ± 0.5

* Navrotsky et al. (1980).
** Clemens et al. (1987), stacking disorder.
† Akaogi and Navrotsky (1985), chain repeat changes.
‡ Robie et al. (1978), TiO_6 tilting transition.

This sensitivity of energy to local environments is reflected in the thermodynamics of order-disorder. A low-symmetry ordered phase often appears only at the final stages of an ordering process. The high-symmetry, long-range disordered phase often contains local environments structurally and energetically almost indistinguishable from those in the low-symmetry, completely ordered phase. The symmetry change, on which crystallographers tend to focus, may thus represent a by-product of, rather than the major driving force for, ordering.

This is illustrated in Figure 16, which shows the enthalpy of ordering of cordierite vs. log time (Carpenter et al., 1983). The linear relation implies that the energy of Si-Al interchange remains constant, and this trend is not perturbed as cordierite proceeds from the disordered hexagonal phase through a set of modulated structures to the fully ordered orthorhombic phase. Furthermore, about 90% of the energy of ordering would be released before an X-ray powder pattern would show any peak splitting indicative of the orthorhombic phase.

A similar picture emerges for Mg_2TiO_4 (Wechsler and Navrotsky, 1984). This inverse spinel undergoes a transition from cubic to a low-temperature tetragonal form, with the ordering of Mg and Ti on octahedral sites. The entropy change at this transition is only 10% of that required for complete octahedral disordering. Substantial short-range order in the cubic high-temperature phase appears to persist several hundred degrees above the transition. The lowering of symmetry thus occurs during the last stages of ordering with decreasing temperature. In $Ba_2In_2O_5$, which is claimed to undergo a disordering of O vacancies, transforming from a brownmillerite structure to disordered perovskite, the entropy change is also $<10\%$ that of the configurational entropy of complete disordering (Prasanna and Navrotsky, 1993). This again implies substantial short-range order in the high-temperature, high-symmetry phase.

Short-range order has a profound effect on the thermodynamics of certain solid solutions. Alumina-rich magnesium aluminates may be considered as solid solutions between spinel and γ alumina or as defect spinels along the $MgAl_2O_4$-$Al_{8/3}O_4$ join. A comparison of the almost zero heats of mixing along this join, measured by

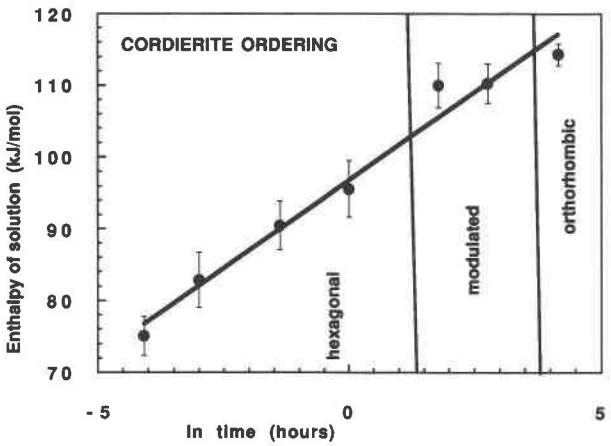

Fig. 16. Enthalpy of solution in molten $2PbO \cdot B_2O_3$ of synthetic cordierite annealed for various times at 1473 K to produce ordering (Carpenter et al., 1983).

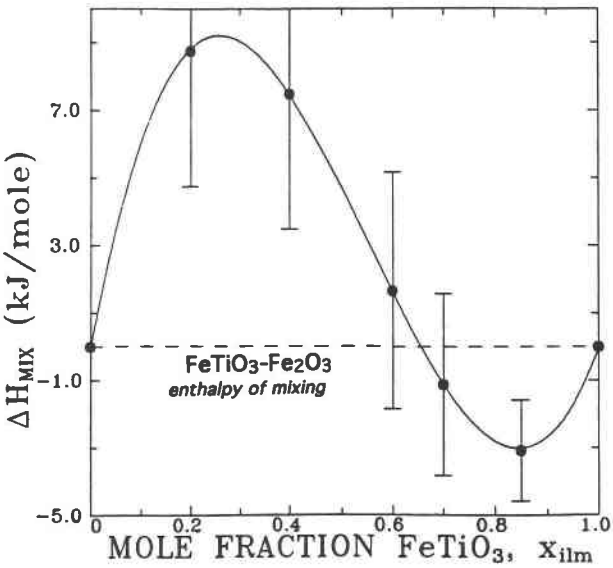

Fig. 17. Enthalpy of mixing in $FeTiO_3$-Fe_2O_3 solid solutions (Brown and Navrotsky, 1994).

calorimetry and the free energies derived from MgO-Al_2O_3 phase equilibria (Navrotsky et al., 1986), suggests that the entropy of mixing is significantly less than that predicted by any simple cation distribution model, indicating considerable short-range order or a correlation between the distribution of Mg and A and that of O vacancies.

Solid solutions with convergent disordering, namely those in which crystallographic sites are distinct only in the ordered phase, are dominated by near-neighbor effects. Typically, in structures where cations order into alternate layers, the thermodynamics reflect a competition of stabilizing interactions between different ions in adjacent layers and destabilizing interactions between different ions within a given layer. The complexity of such behavior is well illustrated by the hematite-ilmenite system, which is so important in iron titanium oxide geothermobarometry.

The Fe_2O_3-$FeTiO_3$ solid-solution series impacts the evolution of igneous and metamorphic rocks in a large number of subsolidus equilibria. Its ubiquitous occurrence with Fe_3O_4-Fe_2TiO_4 solid solutions allows petrologists to estimate temperature and f_{O_2}. In the classical approach, activity-composition relations of Fe_3O_4-Fe_2TiO_4 and Fe_2O_3-$FeTiO_3$ solid solutions are approximated by subregular solution (Margules) formalisms. Data for selected chemical equilibria at a number of temperatures, including ilmenite-hematite and magnetite-ulvöspinel pairs, are then used to determine empirically the Margules parameters (Powell and Powell, 1977; Buddington and Lindsley, 1964; Spencer and Lindsley, 1981; Andersen and Lindsley, 1988; Ghiorso, 1990).

Because of the series expansion nature of this approach, the most common complications affecting the thermodynamic properties of these solid solutions are not easily treated. These complications include cation ordering in both Fe_3O_4-Fe_2TiO_4 and Fe_2O_3-$FeTiO_3$, nonstoichiometry in Fe_3O_4-Fe_2TiO_4 above 1173 K (Taylor, 1964; Schmalzried, 1983; Webster and Bright, 1961; Senderov et al., 1993), and chemical impurities. The most complete attempt to include the effects of cation ordering within the constraints of a simple chemical model is by Ghiorso (1990).

Microscopically based models take into account the cooperative and higher order nature of the order-disorder process in the sesquioxides. The cluster variation method (CVM) invokes interactions out to several neighbors (Burton and Davidson, 1988; Burton, 1984, 1985; Burton and Kikuchi, 1984; Kikuchi, 1977). In this way, structural and thermodynamic parameters are linked. There are, however, drawbacks to such microscopic models. They are mathematically cumbersome and do not lead to closed-form equations for the mixing parameters. Their energetic parameters cannot be uniquely evaluated from phase equilibria alone, and other direct estimates of the energetics of ordering have not been available until recent work (Brown and Navrotsky, 1994).

Evidence for short-range order can be seen in the thermodynamic mixing properties of the $FeTiO_3$-Fe_2O_3 solid-solution series. Measured enthalpies of mixing, ΔH_{mix} (see Fig. 17), show complex behavior (Brown and Navrotsky, 1994). Since both cation ordering and exsolution occur, the mixing enthalpy contains two contributions: a positive term that will drive unmixing, and a negative term that will drive ordering. The positive term dominates in hematite-rich compositions, and the negative in ilmenite-rich.

The entropy of mixing is much smaller than the maximum permitted by the cation distribution (see Fig. 18), which is also suggestive of short-range order. Extensive short-range order is also implied by calorimetry of compositions from $x_{ilm} = 0.6$–0.85 that have different measured cation distributions. Within the resolution of the measurements, the enthalpies of iso-compositional samples with varying cation distributions are indistinguishable.

The implications of such behavior are important in terms of the development of thermodynamic models used to predict the activity-composition relationships at geologically relevant temperatures (673–1173 K). This tem-

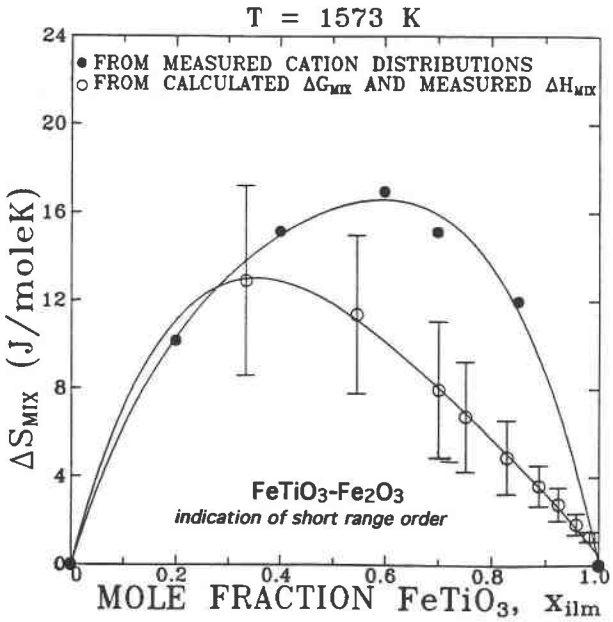

Fig. 18. Entropy of mixing in $FeTiO_3$-Fe_2O_3 solid solutions (Brown and Navrotsky, 1994). Solid circles represent maximum configurational entropy consistent with observed cation distributions and assuming random mixing on each sublattice. Open circles represent entropies of mixing calculated by combining calorimetrically determined enthalpy of mixing with free energy of mixing obtained from phase equilibria.

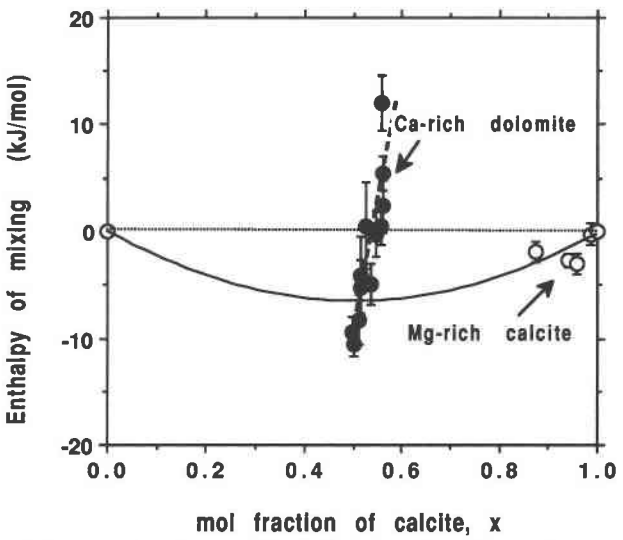

Fig. 19. Enthalpies of formation from $CaCO_3$ and $MgCO_3$ [kJ/mol of $(Mg_{1-x}Ca_x)_2(CO_3)_2$] of Ca-rich dolomite (solid circles) and magnesian calcite (open circles). Data are from Chai et al. (in preparation) and Navrotsky and Capobianco (1987). The horizontal line represents ideal mixing, the solid curve represents possible regular solution behavior of calcite-type solid solution (small negative enthalpy of mixing), and the heavy dashed line represents the trend seen in nonstoichiometric dolomites.

perature range is precisely the range in which significant short-range and long-range ordering (both magnetic and chemical) affects the thermodynamic properties. Paramagnetic to antiferromagnetic transitions in this temperature range occur for compositions from $x_{ilm} = 0$ to 0.4. Chemical ordering also occurs. Further development of cluster variation method or of other structurally based thermodynamic models is necessary. The new calorimetric data contribute to constrain such models.

The ordering that produces dolomite structures from calcite similarly involves the interplay of positive intralayer interactions and negative interlayer interactions (Burton, 1984; Burton and Davidson, 1988; Capobianco et al., 1987; Capobianco and Navrotsky, 1987). In the system $CdCO_3$-$MgCO_3$, both an ordered dolomite phase and a disordered solid solution have been made and studied by solution calorimetry (Capobianco et al., 1987). Positive heats of mixing in the disordered solid solution contrast with the negative heat of formation of the ordered phase, $CdMg(CO_3)_2$ from $CdCO_3$ and $MgCO_3$. Similar behavior is inferred for other carbonate systems (see Table 5). A recent interesting observation (see Fig. 19) is that the energetic stability of the dolomite structure in the system $CaCO_3$-$MgCO_3$ decreases markedly with deviation from the ideal Ca-Mg ratio of unity. Stoichiometric dolomite with 50 mol% $CaCO_3$ has an enthalpy of formation near −11 kJ/mol (Navrotsky and Capobianco, 1987; Chai and Navrotsky, 1993), whereas nonstoichiometric Ca-rich dolomites with 56 mol% $CaCO_3$ have enthalpies of formation close to zero or positive, relative to end-member carbonates (Chai et al., in preparation).

TABLE 5. Enthalpies of formation (kJ/mol) of ordered dolomite phases and disordered solid solutions in carbonates

	Ordered*	Disordered**
$MgCa(CO_3)_2$	−11†	0 to −5†
$MgCd(CO_3)_2$	−5.6‡	+0.9‡
$MnCa(CO_3)_2$	≤−12§	−7.0§

* Formation of ordered stoichiometric dolomite phase from binary carbonates, per mole $AB(CO_3)_2$.
** Formation of disordered 50 mol% solid solution from binary carbonates, per mole $AB(CO_3)_2$.
† Navrotsky and Capobianco (1987); Chai et al. (in preparation).
‡ Capobianco et al. (1987).
§ Capobianco and Navrotsky (1987).

Constraints of short-range order apply to melts and glasses as well. Issues of A avoidance and the applicability of the two-lattice model of mixing entropies in aluminosilicate melts speak to the importance of local ordering (Hon et al., 1981; Henry et al., 1982; Navrotsky, 1986). In several systems showing glass-glass phase separation, clustering on a local scale appears so pervasive that there is little spectroscopic or energetic difference between clear glasses that are considered homogeneous by conventional standards and milky glasses that are phase-separated on a micrometer scale (Ellison and Navrotsky, 1990; Sen et al., 1994). This is interpreted to mean that the short-range order in the clusters is the same in both homogeneous and phase-separated glasses, and

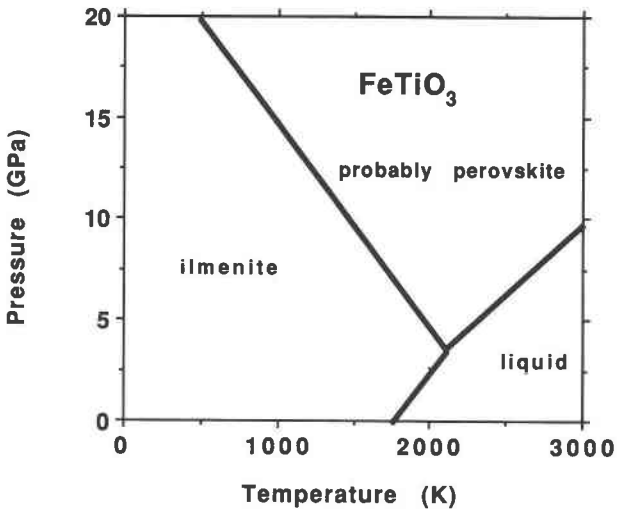

Fig. 20. Phase diagram for $FeTiO_3$ (Mehta et al., 1994).

only the size of the clusters has increased to cause light scattering in the phase-separated glasses.

Structures, like dogs, do not always sit and stay: High-temperature and high-pressure structural states are often not quenchable

High P-T experimentation often relies on examining materials brought to ambient conditions by a quenching procedure that usually involves cooling in a matter of seconds followed by slow depressurization. The materials retrieved sometimes represent the high P-T equilibrium phase, sometimes the low P-T assemblage, and sometimes neither. An example of the latter occurs in high P-T experimentation on ilmenite phases, $MnTiO_3$ and $FeTiO_3$ (Ko et al., 1989; Mehta et al., 1994). In both these systems, the material obtained from experiments quenched in a multianvil apparatus has the lithium niobate structure. However, the lithium niobate form of both compounds transforms rapidly and reversibly to a perovskite in the diamond cell at room temperature and pressures much lower than the initial transformation from ilmenite to lithium niobate. The energetics of the ilmenite to lithium niobate reaction have been measured by calorimetry for both $FeTiO_3$ and $MnTiO_3$. The calorimetric data for $FeTiO_3$ (Mehta et al., 1994) strongly suggest that the observed phase boundary in multianvil experiments is really that between ilmenite and perovskite, with the lithium niobate structure having formed by a rapid, diffusionless transition upon quench (see Fig. 20). The thermochemical data for $MnTiO_3$ are more ambiguous (Ko et al., 1989). The implication of this example is that in-situ structural studies at high pressure and temperature are often the only reliable way of determining what the stable structure under extreme conditions actually is, and that problems in quenching will become more severe as higher pressures are reached. Pressure-induced amorphization, as well as amorphization upon the release of pressure, also involve a complex interplay of stable and metastable reactions.

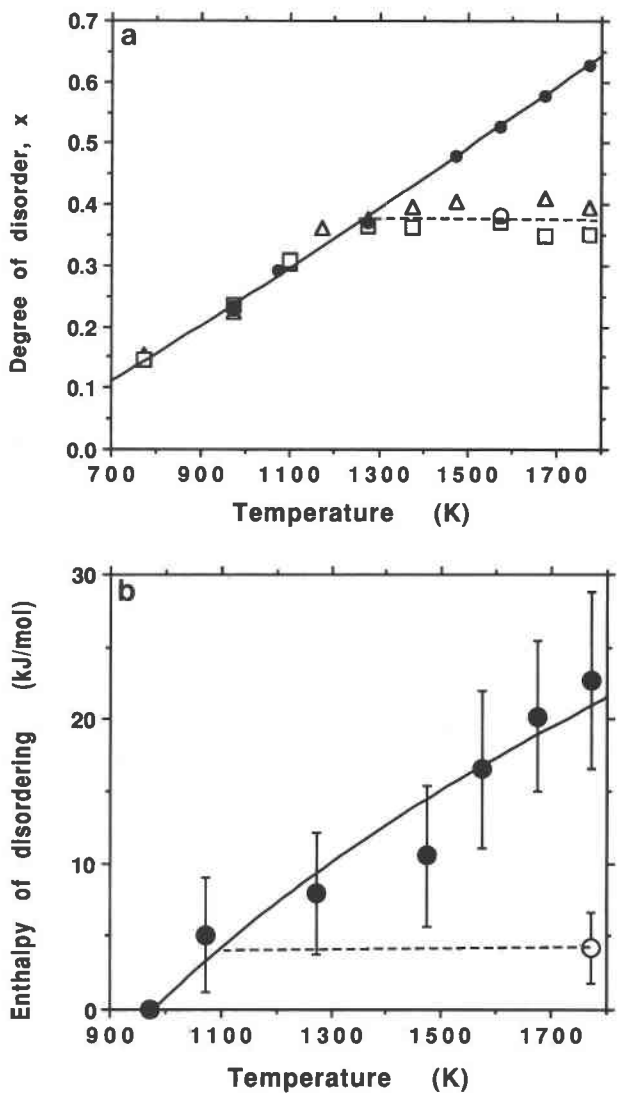

Fig. 21. Energetics of disordering in $MgTi_2O_5$. (**a**) Degree of disorder, x, vs. temperature. Solid circles represent in-situ X-ray measurements of Brown and Navrotsky (1989). Open squares represent X-ray measurements as quenched samples (Brown and Navrotsky, 1989). Open triangles represent X-ray measurements on quenched samples (Wechsler and Navrotsky, 1984). The open circle represents neutron diffraction study of quenched sample (Wechsler and Navrotsky, 1984). The solid curve represents the trend seen in in-situ measurements. The dashed line represents the trend seen in samples quenched from above 1273 K. (**b**) Enthalpy of disordering, relative to sample annealed at 973 K of $MgTi_2O_5$ by in-situ calorimetry (solid circles) (Brown and Navrotsky, 1989) and by calorimetry of a quenched sample (open circle) (Wechsler and Navrotsky, 1984). Solid and dashed lines are as in **a**.

There is increasing evidence that cation distributions in pyroxene, spinel, and pseudobrookite structures are not fully quenchable at atmospheric pressure from tem-

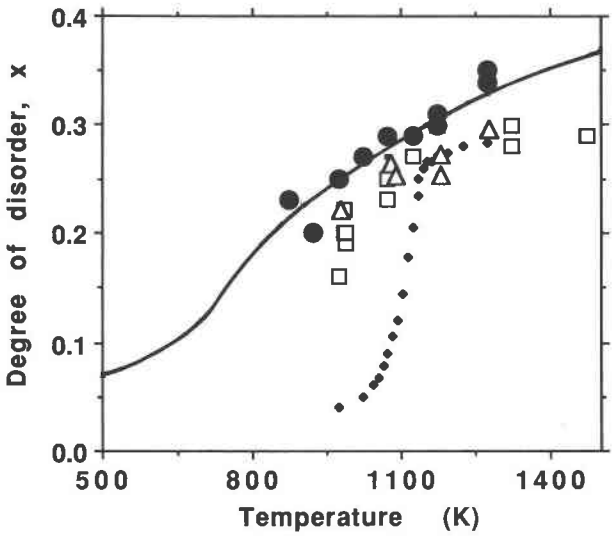

Fig. 22. Cation distribution in $MgAl_2O_4$ spinel (Navrotsky, 1994). Large circles = in-situ neutron diffraction (Peterson et al., 1991). Triangles = NMR on quenched samples (Millard et al., 1992). Squares = NMR on quenched samples (corrected from Wood et al., 1986). Small circles = ESR on heated natural samples (Schmocker and Waldner, 1976). The curve was calculated for ΔH_{int} = 24 kJ.

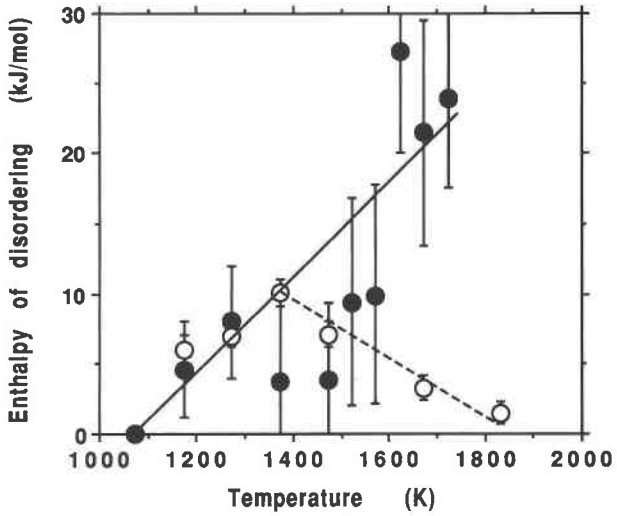

Fig. 23. Enthalpy of disordering, relative to the sample of $NiAl_2O_4$ spinel annealed at 1073 K. Solid circles represent in-situ calorimetric studies (Lysne and Navrotsky, in preparation). Open circles represent calorimetry on quenched samples (Mocala and Navrotsky, 1989). The solid line represents the trend seen in in-situ studies; the dashed line suggests the trend seen in samples quenched from above 1373 K.

peratures above 1273 K. Disorder in the pseudobrookite structure, which contains two in equivalent octahedral sites in a 1:2 ratio, can be treated by the formalism developed for spinels. Two studies of the pseudobrookite, $MgTi_2O_5$ (Wechsler and Navrotsky, 1984; Brown and Navrotsky, 1989), contrasted the behavior of quenched samples with that in situ. The lattice parameters, the cation-site occupancy parameter, and the enthalpy of solution in molten lead borate of quenched samples show a sigmoid dependence on temperature. This suggests that the disordering process reaches some sort of plateau or steady state above 1273 K (see Fig. 21) or that further disordering at higher temperatures is not retained upon quench. The in-situ studies (see Fig. 21) confirm the latter hypothesis by showing a continuous change in lattice parameters, degree of disorder, and enthalpy of disordering when measured directly at high temperature.

Figure 22 shows the results of several studies of the cation distribution in $MgAl_2O_4$ spinel. Quenched samples yield typical sigmoid curves of x vs. T, suggesting that the full extent of disorder above 1273 K is not retained. The one study in situ by neutron diffraction (Peterson et al., 1991) does not go to quite high enough temperature to show definitely that continued disordering does in fact take place at 1273–1600 K, but it does show somewhat more disordered distributions up to 1273 K. For $NiAl_2O_4$, Mocala and Navrotsky (1989) observed a maximum in the enthalpy of disordering as measured on quenched samples (see Fig. 23). Recent work (Lysne and Navrotsky, in preparation) by scanning calorimetry at high temperature shows no maximum but a continued increase in the enthalpy attributable to disordering (see Fig. 23). Once more this suggests that in-situ studies are needed to capture the full extent of disordering reactions above 1273 K.

Conclusions

This review has shown how acid-base reactions, entropy effects, short-range order, and kinetic factors repeatedly affect the thermodynamics of minerals, glasses, and melts. The diversity of examples chosen, which represents only a selection of known systems, suggests that these effects play similar roles in many other cases. Future studies of minerals and ceramics will further elucidate the relations between microscopic and macroscopic and the crystal chemical control of reactions and processes at all scales of time and distance.

Acknowledgments

Without many talented students, postdocs, and collaborators, this work could not have been done. I thank them all. Without the long-term support of the National Science Foundation and the Department of Energy, in both Earth Science and Materials Science, this work would not have been done. I thank the program officers, especially those who helped me get my career started, and the reviewing community. I thank my family and friends, human and canine, for their patience and love. I thank L. Chai and J. Lysne for the use of their unpublished data.

References cited

Akaogi, M., and Navrotsky, A. (1984) Calorimetric study of the stability of spinelloids in the system $NiAl_2O_4$-Ni_2SiO_4. Physics and Chemistry of Minerals, 10, 166–172.

——(1985) Calorimetric study of high-pressure polymorphs of $MnSiO_3$. Physics and Chemistry of Minerals, 12, 317–323.

Akaogi, M., Ito, E., and Navrotsky, A. (1989) Olivine-modified spinel-spinel transitions in the system Mg_2SiO_4-Fe_2SiO_4: Calorimetric measurements, thermochemical calculation, and geophysical application. Journal of Geophysical Research, 94, 15671–15685.

Andersen, D.J., and Lindsley, D.H. (1988) Internally consistent solution

models for Fe-Mg-Mn-Ti oxides: Fe-Ti oxides. American Mineralogist, 73, 714–726.

Brown, N.E., and Navrotsky, A. (1989) Structural, thermodynamic, and kinetic aspects of disordering in the pseudobrookite-type compound, karrooite, $MgTi_2O_5$. American Mineralogist, 74, 902–912.

——— (1994) Hematite-ilmenite (Fe_2O_3-$FeTiO_3$) solid solutions: The effects of cation ordering on the thermodynamics of mixing. American Mineralogist, 79, 485–496.

Buddington, A.F., and Lindsley, D.H. (1964) Iron-titanium oxide minerals and synthetic equivalents. Journal of Petrology, 5, 310–357.

Burton, B.P. (1984) Thermodynamic analysis of the system Fe_2O_3-$FeTiO_3$. Physics and Chemistry of Minerals, 11, 132–139.

——— (1985) Theoretical analysis of chemical and magnetic ordering in the system Fe_2O_3-$FeTiO_3$. American Mineralogist, 70, 1027–1035.

Burton, B.P., and Davidson, P.M. (1988) Multicritical phase relations in minerals. In S. Ghose, J.M.D. Coey, and E. Salje, Eds., Structural and magnetic phase transitions in minerals, p. 60–90. Springer-Verlag, New York.

Burton, B.P., and Kikuchi, R. (1984) The antiferromagnetic transition in Fe_2O_3 in the single prism approximation of the cluster variation method. Physics and Chemistry of Minerals, 11, 125–131.

Capobianco, C., and Navrotsky, A. (1987) Solid solution thermodynamics in $CaCO_3$-$MnCO_3$. American Mineralogist, 72, 312–318.

Capobianco, C., Burton, B.P., Davidson, P.M., and Navrotsky, A. (1987) Structural and calorimetric studies of order-disorder in $CdMg(CO_3)_2$. Journal of Solid State Chemistry, 71, 214–223.

Carpenter, M.A., Navrotsky, A., and McConnell, J.D.C. (1983) Enthalpy effects associated with Al/Si ordering in anhydrous Mg-cordierite. Geochimica et Cosmochimica Acta, 47, 899–906.

Chai, L., and Navrotsky, A. (1993) Thermochemistry of carbonate-pyroxene equilibria. Contributions to Mineralogy and Petrology, 114, 139–147.

Clark, T.V. (1993) Orchestrations 2: Under pressure. Score. Commissioned by Alexandra Navrotsky, president, Mineralogical Society of America, for the 1993 national convention.

Clemens, J.D., Circone, S., Navrotsky, A., McMillan, P.F., Smith, B.K., and Wall, V.J. (1987) Phlogopite: High temperature solution calorimetry, thermodynamic properties, Al-Si and stacking disorder, and phase equilibria. Geochimica et Cosmochimica Acta, 51, 2569–2578.

Duffy, J.A. (1989) A common optical basicity scale for oxide and fluoride glasses. Journal of Non-Crystalline Solids, 109, 35–39.

Duffy, J.A., and Ingram, M.D. (1971a) Establishment of an optical scale for Lewis basicity in inorganic oxyacids, molten salts and glasses. Journal of the American Chemical Society, 93, 6448–6454.

——— (1971b) A new correlation between s-p spectra and the nephelauxetic ratio: Applications in molten salt and glass chemistry. Journal of Chemical Physics, 54, 443–444.

——— (1976) An interpretation of glass chemistry in terms of the optical basicity concept. Journal of Non-Crystalline Solids, 21, 373–410.

Ellison, A.J.G., and Navrotsky, A. (1990) Thermochemistry and structure of model waste glass compositions. In V.M. Oversby and P.W. Brown, Eds., Scientific basis for nuclear waste management. XIII. Materials Research Society Symposium Proceedings, 176, 193–207.

Fei, Y., Saxena, S.K., and Navrotsky, A. (1990) Internally consistent thermodynamic data and equilibrium phase relations in the system MgO-SiO_2 at high pressure and high temperature. Journal of Geophysical Research, 95, 6913–6928.

Geisinger, K.L., Gibbs, G.V., and Navrotsky, A. (1985) A molecular orbital study of bond length and angle variation in framework silicates. Physics and Chemistry of Minerals, 11, 266–283.

Gerardin, C., Sundaresan, S., Benziger, J., and Navrotsky, A. (1994) Structural investigation and energetics of mullite formation from sol-gel precursors. Chemistry of Materials, in press.

Ghiorso, M.S. (1990) Thermodynamic properties of hematite-ilmenite-geikielite solid solutions. Contributions to Mineralogy and Petrology, 104, 645–667.

Gibbs, G.V. (1982) Molecules as models for bonding in silicates. American Mineralogist, 67, 421–450.

Henry, D.J., Navrotsky, A., and Zimmermann, H.D. (1982) Thermodynamics of plagioclase-melt equilibria in the system albite-anorthite-diopside. Geochimica et Cosmochimica Acta, 46, 381–391.

Hon, R., Henry, D.J., Navrotsky, A., and Weill, D.F. (1981) A thermochemical calculation of the pyroxene saturation surface in the system diopside-albite-anorthite. Geochimica et Cosmochimica Acta, 45, 157–161.

Ito, E., Akaogi, M., Topor, L., and Navrotsky, A. (1990) Negative *P-T* slopes for reactions forming $MgSiO_3$ perovskite confirmed by calorimetry. Science, 249, 1275–1278.

Kieffer, S.W. (1979a) Thermodynamics and lattice vibrations of minerals. I. Mineral heat capacities and their relationships to simple lattice vibrational models. Reviews of Geophysics and Space Physics, 17, 1–19.

——— (1979b) Thermodynamics and lattice vibrations of minerals. II. Vibrational characteristics of silicates. Reviews of Geophysics and Space Physics, 17, 20–34.

——— (1979c) Thermodynamics and lattice vibrations of minerals. III. Lattice dynamics and an approximation for minerals with application to simple substances and framework silicates. Reviews of Geophysics and Space Physics, 17, 35–59.

——— (1979d) Thermodynamics and lattice vibrations of minerals. IV. Application to chain and sheet silicates and orthosilicates. Reviews of Geophysics and Space Physics, 18, 862–886.

——— (1982) Thermodynamics and lattice vibrations of minerals. V. Applications to phase equilibria, isotopic fractionation, and high-pressure thermodynamic properties. Reviews of Geophysics and Space Physics, 20, 827–849.

Kikuchi, R. (1977) The cluster variation method. Journal of Physics, C7, (suppl. 12, tome 38), 307–313.

Ko, J., Brown, N.E., Navrotsky, A., Prewitt, C.T., and Gasparik, T. (1989) Phase equilibrium and calorimetric study of the transition of $MnTiO_3$ from the ilmenite to the lithium niobate structure and implications for the stability field of perovskite. Physics and Chemistry of Minerals, 16, 727–733.

Leinenweber, K., and Navrotsky, A. (1989) Thermochemistry of phases in the system $MgGa_2O_4$-Mg_2GeO_4. Physics and Chemistry of Minerals, 16, 497–502.

Mehta, A., Leinenweber, K., and Navrotsky, A. (1994) Calorimetric study of high pressure polymorphism in $FeTiO_3$: Stability of the perovskite phase. Physics and Chemistry of Minerals, in press.

Millard, R.L., Peterson, R.C., and Hunter, B.K. (1992) Temperature dependence of cation disorder in $MgAl_2O_4$ spinel using ^{27}Al and ^{17}O magic-angle spinning NMR. American Mineralogist, 77, 44–52.

Mocala, K., and Navrotsky, A. (1989) Structural and thermodynamic variation in nickel aluminate spinel. Journal of the American Ceramic Society, 12, 826–832.

Mocala, K., Navrotsky, A., and Sherman, D.M. (1992) High temperature heat capacity of Co_3O_4 spinel: Thermally induced spin unpairing transition. Physics and Chemistry of Minerals, 19, 88–95.

Navrotsky, A. (1971) Thermodynamics of formation of the silicates and germanates of some divalent transitions metals and of magnesium. Journal of Inorganic and Nuclear Chemistry, 33, 4035–4050.

——— (1974) Thermodynamics of binary and ternary transition metal oxides in the solid state. In D.W.A. Sharp, Ed., MTP International Reviews of Science, inorganic chemistry, series 2, vol. 5, p. 29–70. Butterworths-University Park Press, Baltimore, Maryland.

——— (1975) Thermodynamics of formation of some compounds with the pseudobrookite structure of the $FeTi_2O_5$-Ti_3O_5 solid solution series. American Mineralogist, 60, 249–256.

——— (1980) Lower mantle phase transitions may generally have negative pressure-temperature slopes. Journal of Geophysical Research Letters, 7, 709–711.

——— (1986) Thermodynamics of silicate glasses and melts. In C.M. Scarfe, Ed., Mineralogical Association of Canada Short Course in Silicate Melts, 12, 130–153.

——— (1988) Experimental studies of mineral energetics. In E. Salje, Ed., Physical properties and thermodynamic behaviour of minerals, p. 403–432. Reidel, Dordrecht, The Netherlands.

——— (1994) Physics and chemistry of Earth materials. Cambridge University Press, New York, in press.

Navrotsky, A., and Capobianco, C. (1987) Enthalpies of formation of dolomite and of magnesian calcites. American Mineralogist, 72, 782–787.

Navrotsky, A., and Kleppa, O.J. (1967) The thermodynamics of cation distributions in simple spinels. Journal of Inorganic and Nuclear Chemistry, 29, 2701–2714.

——— (1968) Thermodynamics of formation of simple spinels. Journal of Inorganic and Nuclear Chemistry, 30, 479–498.
——— (1969) Enthalpies of formation of some tungstates MWO_4. Inorganic Chemistry, 8, 756–758.
Navrotsky, A., Hon, R., Weill, D.F., and Henry, D.J. (1980) Thermochemistry of glasses and liquids in the systems $CaMgSi_2O_6$-$CaAl_2Si_2O_8$-$NaAlSi_3O_8$, SiO_2-$CaAl_2Si_2O_8$-$NaAlSi_3O_8$ and SiO_2-$A1_2O_3$-CaO-Na_2O. Geochimica et Cosmochimica Acta, 44, 1409–1423.
Navrotsky, A., Peraudeau, G., McMillan, P., and Coutures, J.P. (1982) A thermochemical study of glasses along the joins silica-calcium aluminate and silica-sodium aluminate. Geochimica et Cosmochimica Acta, 46, 2039–2047.
Navrotsky, A., Geisinger, K.L., McMillan, P., and Gibbs, G.V. (1985) The tetrahedral framework in glasses and melts: Inferences from molecular orbital calculations and implications for structure, thermodynamics, and physical properties. Physics and Chemistry of Minerals, 11, 284–298.
Navrotsky, A., Wechsler, B.A., Geisinger, K., and Seifert, F. (1986) Thermochemistry of $MgAl_2O_4$-$Al_{8/3}O_4$ defect spinels. Journal of the American Ceramic Society, 69, 418–422.
Navrotsky, A., Ziegler, D., Oestrike, R., and Maniar, P. (1989) Calorimetry of silicate melts at 1773 K: Measurement of enthalpies of fusion and of mixing in the systems diopside-anorthite-albite and anorthite-forsterite. Contributions to Mineralogy and Petrology, 101, 122–130.
O'Neill, H.St.C., and Navrotsky, A. (1983) Simple spinels: Crystallographic parameters, cation radii, lattice energies, and cation distributions. American Mineralogist, 68, 181–194.
——— (1984) Cation distributions and thermodynamic properties of binary spinel solid solutions. American Mineralogist, 69, 733–755.
Ottonello, G. (1987) Energies and interactions in binary (*Pbnm*) orthosilicates: A born parameterization. Geochimica et Cosmochimica Acta, 51, 3119–3135.
Peterson, R.C., Lager, G.A., and Hitterman, R.L. (1991) A time-of-flight neutron powder diffraction study of $MgAl_2O_4$ at temperatures up to 1273 K. American Mineralogist, 76, 1455–1458.
Powell, R., and Powell, M. (1977) Geothermometry and oxygen barometry using coexisting iron-titanium oxides: A reappraisal. Mineralogical Magazine, 41, 257–263.
Prasanna, T.R.S., and Navrotsky, A. (1993) Energetics of the oxygen vacancy order-disorder transition in $Ba_2In_2O_5$. Journal of Materials Research, 8, 1464–1466.
——— (1994) Energetics of brownmillerite-perovskite pseudobinary $Ca_2Fe_2O_5$-$CaTiO_3$. Journal of Materials Research, in press.
Reznitskiy, L.A. (1986) Crystal energies of structural fragments and the thermochemical properties of simple and multicomponent oxides. Geochemistry International, 23, 50–60.
Robie, R.A., Hemingway, B.S., and Fisher, J.R. (1978) Thermodynamic properties of minerals and related substance at 298.15 K and 1 bar (10^5 Pascals) pressure and at higher temperatures. U.S. Geological Survey Bulletin, 1452, 456 p.
Robinson, G.R., Jr., and Haas, J.L., Jr. (1983) Heat capacity, relative enthalpy, and calorimetric entropy of silicate minerals: An empirical method of prediction. American Mineralogist, 68, 541–553.
Roy, B.N., and Navrotsky, A. (1984) Thermochemistry of charge-coupled substitutions in silicate glasses: The systems $M_{1/n}^{n+}AlO_2$-SiO_2 (M = Li, Na, K, Rb, Cs, Mg, Ca, Sr, Ba, Pb). Journal of the American Ceramic Society, 67, 606–610.
Schmalzried, H. (1983) Thermodynamics of compounds with narrow ranges of nonstoichiometry. Berichte der Bunsen-Gesellschaft für physikalische Chemie, 87, 726–733.
Schmocker, U., and Waldner, F. (1976) The inversion parameter with respect to the space group of $MgAl_2O_4$ spinels. Journal of Physics C: Solid State Physics, 9, L235–L237.
Sen, S., Gerardin, C., Navrotsky, A., and Dickinson, J.E. (1994) Energetics and structural changes associated with phase separation and crystallization in lithium silicate glasses. Journal of Non-Crystalline Solids, in press.
Senderov, E., Dogan, A.U., and Navrotsky, A. (1993) Nonstoichiometry of magnetite-ulvöspinel solid solutions quenched from 1300 °C. American Mineralogist, 78, 565–573.
Shannon, R.D. (1976) Revised effective ionic radii and systematic studies of interatomic distances in halides and chalcogenides. Acta Crystallographica, A32, 751–767.
Spencer, K.J., and Lindsley, D.H. (1981) A solution model for coexisting iron-titanium oxides. American Mineralogist, 66, 1189–1201.
Tardy, Y., and Garrets, R.M. (1974) A method of estimating the Gibbs energies of formation of layer silicates. Geochimica et Cosmochimica Acta, 88, 1101–1116.
Taylor, R.W. (1964) Phase equilibria in the system FeO-Fe_2O_3-TiO_2 at 1300 °C. American Mineralogist, 49, 1016–1030.
Webster, A.H., and Bright, N.F.H. (1961) The system iron-titanium-oxygen at 1200 °C and partial oxygen pressures between 1 atm and 2×10^{-14} atm. Journal of the American Ceramic Society, 44, 110–116.
Wechsler, A., and Navrotsky, A. (1984) Thermodynamics and structural chemistry of compounds in the system MgO-TiO_2. Journal of Solid State Chemistry, 55, 165–180.
Wood, B.J., Kirkpatrick, R.J., and Montez, B. (1986) Order-disorder phenomena in $MgAl_2O_4$ spinel. American Mineralogist, 71, 999–1006.

Manuscript received January 24, 1994
Manuscript accepted March 16, 1994

Appendix 1. Musical interlude

A short musical piece for solo flute was part of the Presidential Address. The composition, titled "Orchestrations 2: Under Pressure" is a work of Saint Louis composer Timothy Vincent Clark, who is known nationally for his work with the new music ensemble Synchronia and within Saint Louis as the new and classical music critic for the *Riverfront Times*. Clark explained: "The original title, 'Under Pressure,' makes reference to one type of ongoing mineralogical research. A mineral is forced, under great pressure similar to that found in the Earth's mantle, to realign and compress its atoms, resulting in a new, dense, crystalline structure. Pressure and pitch realignment are a strong feature of the work. Yet, as the composing proceeded, I also realized I was employing an instrumental strategy similar to one I used for a 1983 solo piano work: I was orchestrating the material for the large variety of sounds available to the flute. So, borrowing from the piano title, I added 'Orchestrations 2' as a further indication of the sense of the work."

The work is constructed around three interlocking symmetrical structures: a perfect-fifth pairing, A-E/A-D; a paired expansion by thirds, A-C-E/A-F#-D; and a whole-step centering process, C-D/E-D. Each of these focus pitches is accompanied by its own particular universe of intervallic associations (or, if you wish, its own particular group of orbiting electrons). The pitch A, the starting point for two of the structures and the focus of most of the rapid activity, represents the mineral in a state of excitation, whereas the frozen material surrounding the process-concluding pitch D at the close of the work represents the crystalline structures. Appendix Figure 1 shows a portion of the score.

My motivations for commissioning this piece were varied. The flutist, Betsy Feldman, a good friend, provided the impetus and played the world premiere on October 26, 1993. We first thought of music designed around pure, almost mathematical or crystalline forms. Bach and Varese quickly came to mind. But then MSA is doing new, now research—why shouldn't it get new, now music as well? We decided it's important, and fun, for MSA to be exposed to the ideas and thinking of other disciplines, and to learn—and in this case, hear—what musicians can do with ideas drawn from mineralogical research. "Orchestrations 2: Under Pressure" was the result of this brainstorm.

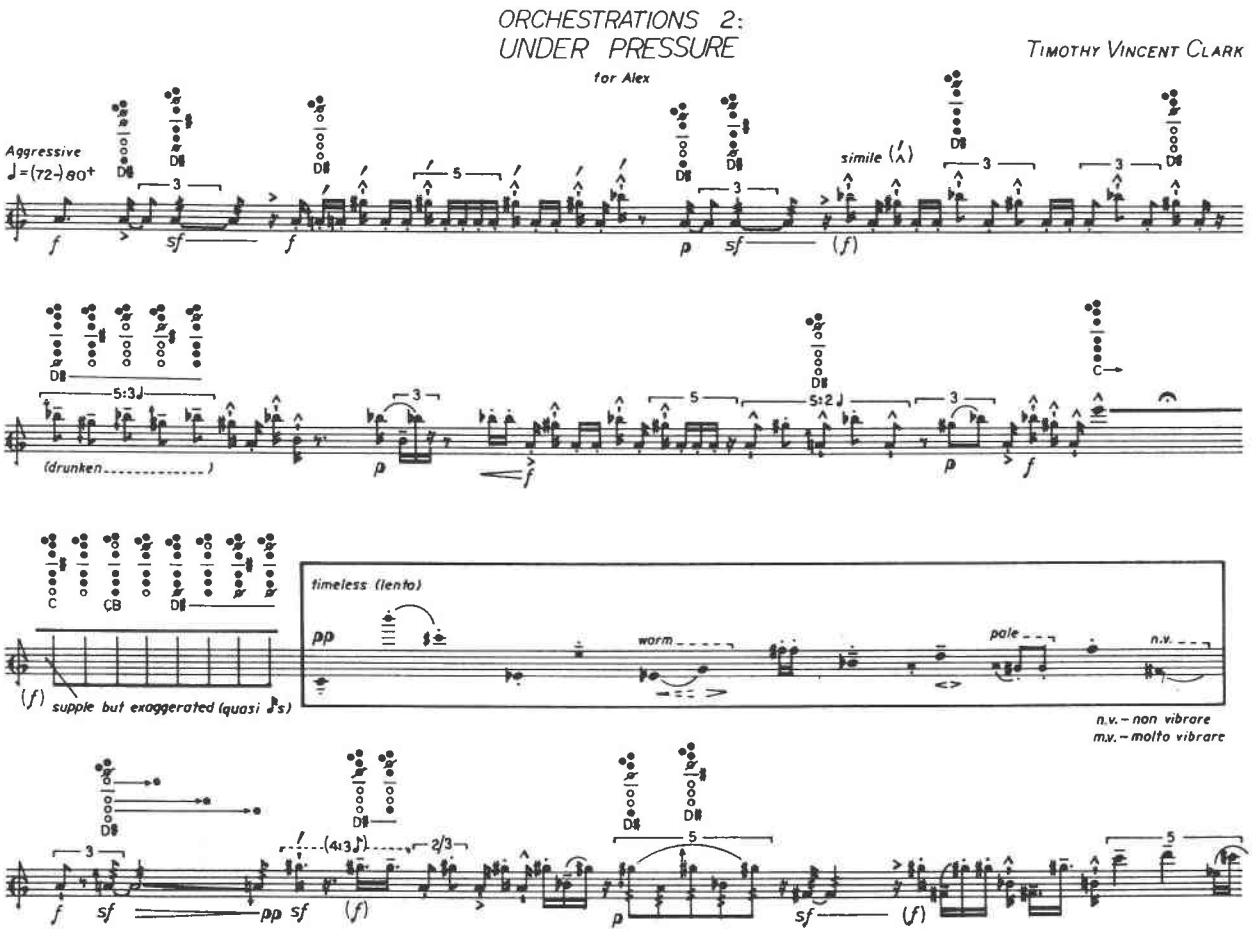

Appendix Fig. 1. Portions of the score of "Orchestrations 2: Under Pressure." Copyright 1993 by Timothy Vincent Clark. All rights reserved. Commissioned by Alexandra Navrotsky, president, Mineralogical Society of America, for the 1993 national convention.